

# Sinking deltas due to human activities

James P. M. Syvitski<sup>1\*</sup>, Albert J. Kettner<sup>1</sup>, Irina Overeem<sup>1</sup>, Eric W. H. Hutton<sup>1</sup>, Mark T. Hannon<sup>1</sup>, G. Robert Brakenridge<sup>2</sup>, John Day<sup>3</sup>, Charles Vörösmarty<sup>4</sup>, Yoshiki Saito<sup>5</sup>, Liviu Giosan<sup>6</sup> and Robert J. Nicholls<sup>7</sup>

**Many of the world's largest deltas are densely populated and heavily farmed. Yet many of their inhabitants are becoming increasingly vulnerable to flooding and conversions of their land to open ocean. The vulnerability is a result of sediment compaction from the removal of oil, gas and water from the delta's underlying sediments, the trapping of sediment in reservoirs upstream and floodplain engineering in combination with rising global sea level. Here we present an assessment of 33 deltas chosen to represent the world's deltas. We find that in the past decade, 85% of the deltas experienced severe flooding, resulting in the temporary submergence of 260,000 km<sup>2</sup>. We conservatively estimate that the delta surface area vulnerable to flooding could increase by 50% under the current projected values for sea-level rise in the twenty-first century. This figure could increase if the capture of sediment upstream persists and continues to prevent the growth and buffering of the deltas.**

Close to half a billion people live on or near deltas, often in megacities<sup>1,2</sup>. Twentieth-century catchment developments, and population and economic growth have had a profound impact on deltas<sup>3</sup>. As a result, these environments and their populations are under a growing risk of coastal flooding, wetland loss, shoreline retreat and loss of infrastructure<sup>4,5</sup>. More than 10 million people a year experience flooding due to storm surges alone, and most of these people are living on Asian deltas<sup>6</sup>. Flooding may originate from intense precipitation directly onto a delta, from river overbanking or from hurricane-induced storm surges.

Using globally consistent and high-resolution satellite data, 33 representative deltas (see Supplementary Fig. S1) were examined to ascertain their proclivity to flooding and to see why they are sinking more rapidly than global sea level is rising. Each delta's topography in relation to mean sea level was determined from Shuttle Radar Topography Mission (SRTM) data (Figs 1–3). Historical maps published between 1760 and 1922 (Supplementary Fig. S9) were geo-referenced against the topographic data to ascertain how the river channels shifted their location and pattern across each of the deltas before the heavy imprint of modern civilization. Visible and near-infrared images from the Moderate Resolution Imaging Spectroradiometer (MODIS) satellite were used to establish the extent of recent flooding on the deltas, whether the flooding was from river runoff or from coastal storm surges, and whether the floodwaters carried suspended sediment (Supplementary Figs S2–S8). These data, combined with trends found in river-load and sea-level data, were used to determine whether modern delta plains are keeping up with rising sea levels by adding new sediment layers to their surface during periods of flooding.

## Controls on delta surface elevation

Vertical change in delta surfaces relative to local mean sea level,  $\Delta_{\text{RSL}}$ , is determined by five factors:  $\Delta_{\text{RSL}} = A - \Delta E - C_N - C_A \pm M$ .

A delta's aggradation rate ( $A$ ) is determined from the volume of sediment delivered to and retained on the subaerial delta surface as new sedimentary layers. Sediment delivery is highly dynamic and occurs as a hierarchy of pulses over a wide range of temporal and spatial scales<sup>7</sup>. The value of  $A$  typically varies from 1 to 50 mm yr<sup>-1</sup> (Table 1). Most river floods bring large amounts of sediment to a delta's surface, although modern dam interception of upstream river-borne sediment may leave a river with relatively clean water, and with flows of reduced magnitude. Furthermore, the use of artificial levees combined with reductions in the number of distributary channels can prohibit river flooding onto the delta plain. Flooding from ocean surges may still contribute turbid water. For example, hurricane-generated surges have added marine sediment to the outer portions of the Mississippi Delta<sup>8,9</sup>.

The quantity  $\Delta E$  is the eustatic sea-level rate determined from changes to the volume of the global ocean over time, as influenced by fluctuations in the storage of terrestrial water (for example glaciers, ice sheets, groundwater, lakes and reservoirs) and fluctuations in ocean water expansion due to water temperature changes. Today  $\Delta E$  is positive and contributes around 1.8 to 3 mm yr<sup>-1</sup> (refs 10,11) under the anthropogenic influence of global warming. The Intergovernmental Panel on Climate Change (IPCC) projects that sea level will rise by another 21 to 71 cm by 2070, with a best estimate of 44 cm averaged globally<sup>10</sup>; researchers are working to determine whether the major ice sheets might contribute even more water over this period and how  $\Delta E$  varies spatially owing to gravimetric effects<sup>12</sup>.

Natural compaction ( $C_N$ ) and accelerated compaction ( $C_A$ ) reduce the volume of deltaic deposits. Natural compaction involves natural changes in the void space within sedimentary layers (for example dewatering, grain-packing realignment and organic matter oxidation)<sup>13,14</sup> and is typically  $\leq 3$  mm yr<sup>-1</sup> (ref. 5). Accelerated compaction is the anthropogenic contribution to volume change as a consequence of subsurface mining (oil, gas or groundwater),

<sup>1</sup>CSDMS Integration Facility, INSTAAR, University of Colorado, Boulder, Colorado 80309-0545, USA, <sup>2</sup>Dartmouth Flood Observatory, Dartmouth College, Hanover, New Hampshire 03755, USA, <sup>3</sup>Department of Oceanography and Coastal Sciences, Louisiana State University, Baton Rouge, Louisiana 70803, USA, <sup>4</sup>Department of Civil Engineering, City College of New York, City University of New York, New York 10035, USA, <sup>5</sup>Geological Survey of Japan, AIST, Tsukuba 305-8567, Japan, <sup>6</sup>Woods Hole Oceanographic Institution, Woods Hole, Massachusetts 02543, USA, <sup>7</sup>School of Civil Engineering and the Environment and Tyndall Centre for Climate Change Research, University of Southampton, SO17 1BJ, UK.

\*e-mail: James.syvitski@colorado.edu

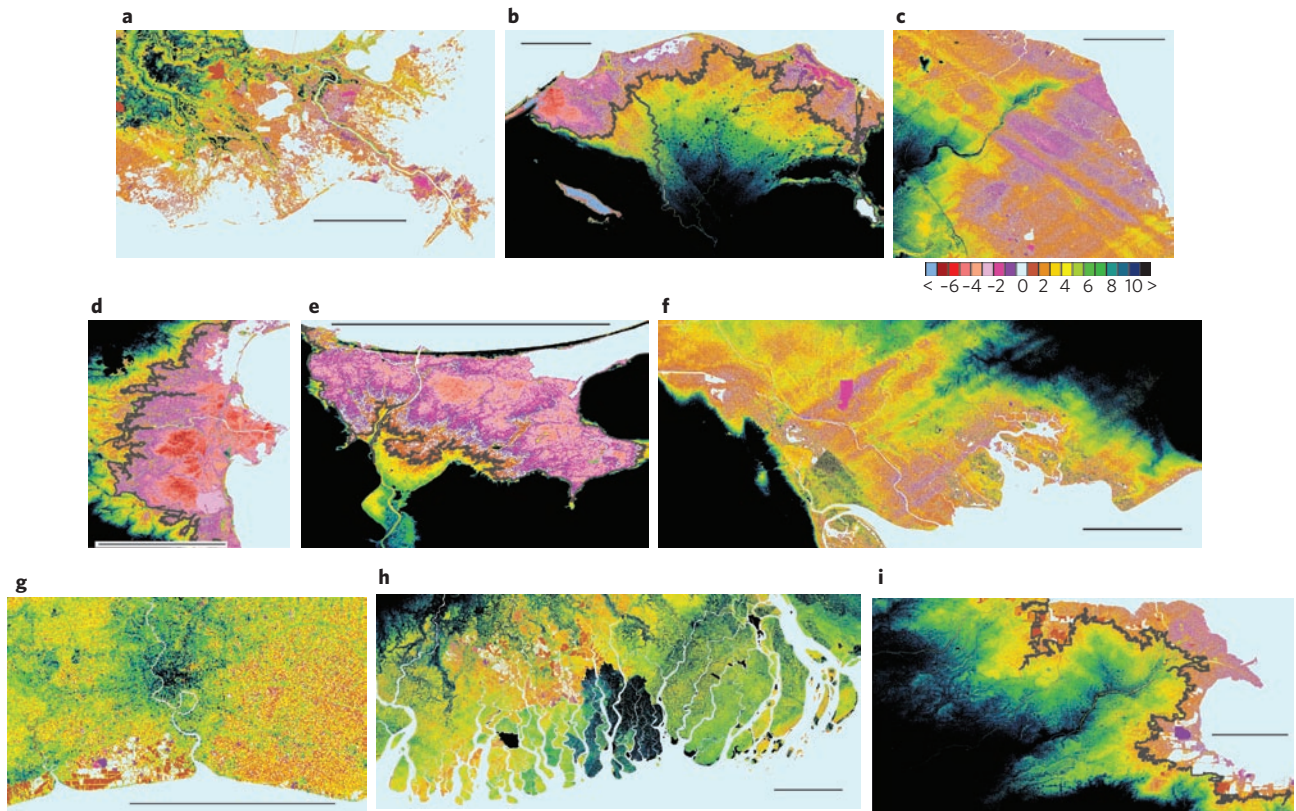


**Figure 1 | Topography of representative deltas.** SRTM altimetry is binned at 1-m vertical intervals, starting at sea level (light blue), to a height of 10 m, then black. Topography below mean sea level is in shades of pink. **a**, Mississippi, USA; **b**, Nile, Egypt; **c**, old abandoned Yellow, China; **d**, Po, Italy; **e**, Vistula, Poland; **f**, Shatt al Arab, Iraq; **g**, Chao Phraya, Thailand; **h**, Ganges-Brahmaputra, Bangladesh; and **i**, modern (since 1855) Yellow, China. Scale bar on images represents 50 km. For **b**, **d**, **e** and **i** examples, the 2-m best-fit isoline is provided as a grey line.

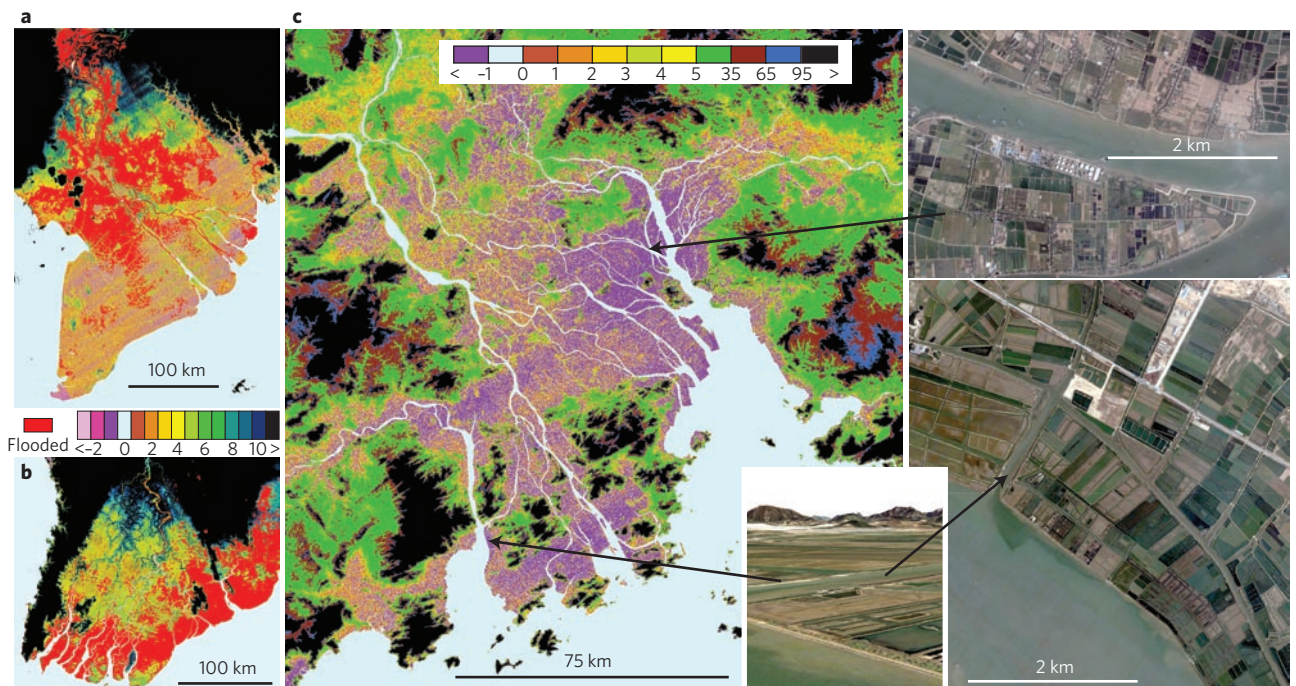


**Figure 2 | Examples of actual and potential delta flooding.** **a**, Mekong, Vietnam, and **b**, Irrawaddy, Myanmar, displayed with SRTM altimetry, showing flooded areas in dark red, based on MODIS imaging. The Mekong River flooded on 8 November 2007. A coastal surge from Cyclone Nargis inundated the Irrawaddy on 5 May 2008. **c**, The Pearl Delta, China, displayed with SRTM altimetry, with areas below sea level shown in purple. The Pearl is protected from storm surges by coastal and channel barriers as seen in associated Digital Globe images (Google Earth).



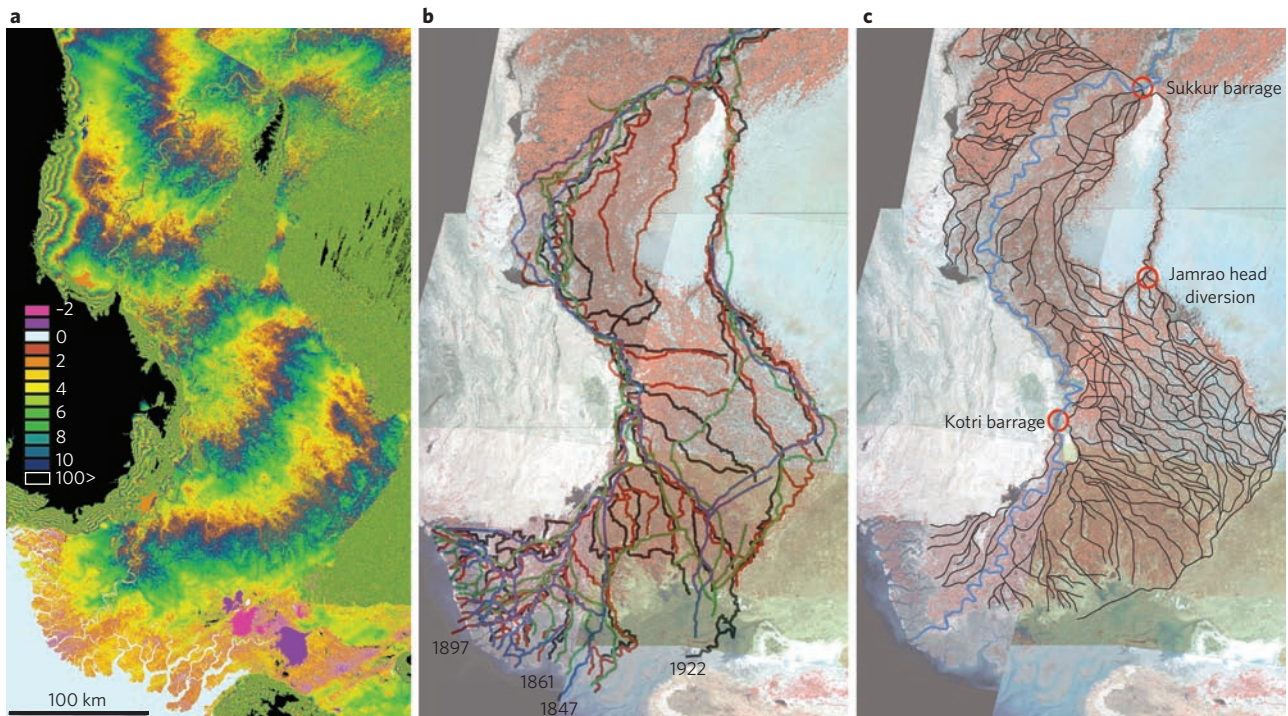


**Figure 3 | The Indus floodplain and delta (Pakistan).** **a**, SRTM altimetry, binned at 1-m vertical intervals, starting at sea level (light blue), then one colour per 1-m interval, with colours cycled every 10 m, to a height of 100 m, then black. Topography below mean sea level is in shades of pink. **b**, Historical location of distributary channels (colour, year): blue, 1847; green, 1861; red, 1897; black, 1922. **c**, Modern irrigation channel system with main water distribution stations. Only one channel (blue) now carries significant water to the ocean.

human-influenced soil drainage and accelerated oxidation, and can exceed natural compaction by an order of magnitude;  $C_A$  on the Chao Phraya Delta has ranged from 50 to 150 mm yr<sup>-1</sup> as a result of groundwater withdrawal<sup>15</sup>. The Po Delta subsided 3.7 m in the twentieth century, 81% of which is attributed to methane mining<sup>16</sup>.

The quantity  $M$  is the typically downward vertical movement of the land surface as influenced by the redistribution of Earth's masses (for example sea-level fluctuations<sup>17</sup>, growth of delta deposits<sup>18</sup>, growth or shrinkage of nearby ice masses<sup>19</sup>, tectonics<sup>20</sup> and deep-seated thermal subsidence<sup>21</sup>). The movement is highly variable spatially, but rates are typically between 0 and -5 mm yr<sup>-1</sup> (refs 5, 20).

Field measurements often do not separate a delta's overall subsidence,  $S$  (relative sinking of the land surface), into its components  $M$ ,  $C_N$  and  $C_A$ . Furthermore,  $\Delta_{RSL}$  rates are often measured directly and the unique contributions of  $S$  and  $\Delta E$  are not even separated. Large deltas (10<sup>4</sup> to 10<sup>5</sup> km<sup>2</sup> or more) have spatially variable subsidence that depends on a location's unique load and compaction history<sup>22</sup>. Seldom is a delta-integrated  $S$  calculated. In one rare study, involving the Mississippi Delta, three independent data sources (synthetic aperture radar, global positioning system geodesy and levelling) determined an area-averaged  $S$  of 5 to 6 mm yr<sup>-1</sup>. The survey included parts of New Orleans that have subsided 25 mm yr<sup>-1</sup> since 1850 when large-scale drainage and levee construction began<sup>23</sup>.

Unique to this study are our estimates of spatially averaged aggradation rates for 33 representative deltas, both before and after substantive human intervention. We first estimate early-twentieth-century aggradation rates (Table 1) from observed sediment loads that once reached the deltas as measured before the proliferation of upstream dams and downstream discharge diversions<sup>24–26</sup>, and from the amount of this sediment that is retained on a delta per unit area, based on model estimates<sup>1</sup>. Retention rates vary from 10–20% for small, steep-gradient rivers to 50–60%

for large deltas with numerous distributary channels. Modern (twenty-first-century) aggradation rates (Table 1) are then adjusted for late-twentieth-century sediment reduction caused by reservoir trapping and engineering controls across a delta. We can compare aggradation with published subsidence values (see for example refs 15, 24), and  $\Delta_{RSL}$  rates determined from the Permanent Service for Mean Sea Level (PSMSL) gauging records (Supplementary Table S1). Unfortunately published subsidence rates are often local maximum rates within a delta and  $\Delta_{RSL}$  is determined from tide gauges that simply represent a local value, whereas our reconstructed aggradation rates are spatially averaged.

### Changes in modern delta aggradation

We find that sediment delivery to deltas has been reduced or eliminated at all scales<sup>7</sup>. Table 1 lists the sediment reduction due to upstream damming over the past 50 years.

Daily satellite imagery of deltas has been available for only the past decade, too short an interval to confirm the full extent of flooding (Supplementary Information). Imagery for this period shows that most deltas have experienced coastal inundation from surges, floods from rivers overbanking their levees, flooding from intense rainfall within the delta, or all three sources of flooding (Table 1). In 2007–08 alone, the following deltas experienced substantial flooding: Ganges, Mekong (Fig. 2), Irrawaddy (Fig. 2), Chao Phraya, Brahmani, Mahanadi, Krishna and Godavari (Supplementary Figs S2–S8), with more than 100,000 lives lost and more than a million habitants displaced. Some of the deltas (Ganges, Mahanadi, Mekong and Irrawaddy) did receive river-borne or marine-borne sediment added to their surface, but most of the deltas that suffered from floods did not receive a significant input of sediment (Table 1; Supplementary Figs S2–S8), and this lack of sediment can be attributed to upstream damming.

Another factor that reduces delta aggradation is that the number of active distributary channels has been reduced to support

**Table 1 | Representative deltas with key environment data. Storm surge, river (distributary) channel, and precipitation (*in situ*) flooding are from MODIS satellite data since 2000. The level of sediment-load reduction is across the twentieth century, as is the reduction in distributary and subsurface mining. Rates of relative sea-level rise are time-variable and the ranges provided cover either different times or different areas of a delta.**

Delta	Area < 2 m above sea level (km <sup>2</sup> )	Storm-surge area (km <sup>2</sup> )*	Recent area of river flooding (km <sup>2</sup> )	Recent area of <i>in situ</i> flooding (km <sup>2</sup> )	Sediment reduction (%)	Floodplain or delta flow diversion	Distributary channel reduction (%)	Subsurface water, oil and gas mining	Early-twentieth-century aggradation rate (mm yr <sup>-1</sup> )	Twenty-first-century aggradation rate (mm yr <sup>-1</sup> )	Relative sea-level rise (mm yr <sup>-1</sup> )
<b>Deltas not at risk: aggradation rates unchanged, minimal anthropogenic subsidence</b>											
Amazon, Brazil	1,960 <sup>†</sup>	0; LP	0	9,340	0	No	0	0	0.4	0.4	Unknown
Congo <sup>‡</sup> , DRC	460	0; LP	0	0	20	No	0	0	0.2	0.2	Unknown
Fly, Papua New Guinea	70 <sup>†</sup>	0; MP	140	280	0	No	0	0	5	5	0.5
Orinoco, Venezuela	1,800 <sup>†</sup>	0; MP	3,560	3,600	0	No	0	Unknown	1.3	1.3	0.8–3
Mahaka, Borneo	300	0; LP	0	370	0	No	Unknown	0	0.2	0.2	Unknown
<b>Deltas at risk: reduction in aggradation, but rates still exceed relative sea-level rise</b>											
Amur, Russia	1,250	0; LP	0	0	0	No	0	0	2	1.1	1
Danube, Romania	3,670	1,050	2,100	840	63	Yes	0	Minor	3	1	1.2
Han, Korea	70	60	60	0	27	No	0	0	3	2	0.6
Limpopo, Mozambique	150	120	200	0	30	No	0	0	7	5	0.3
<b>Deltas at greater risk: reduction in aggradation where rates no longer exceed relative sea-level rise</b>											
Brahmani, India	640	1,100	3,380	1,580	50	Yes	0	Major	2	1	1.3
Godavari, India	170	660	220	1,100	40	Yes	0	Major	7	2	~3
Indus, Pakistan	4,750	3,390	680	1,700	80	Yes	80	Minor	8	1	>1.1
Mahanadi, India	150	1,480	2,060	1,770	74	Yes	40	Moderate	2	0.3	1.3
Parana, Argentina	3,600	0; LP	5,190	2,600	60	No	Unknown	Unknown	2	0.5	2–3
Vistula, Poland	1,490	0; LP	200	0	20	Yes	75	Unknown	1.1	0	1.8
<b>Deltas in peril: reduction in aggradation plus accelerated compaction overwhelming rates of global sea-level rise</b>											
Ganges <sup>‡</sup> , Bangladesh	6,170 <sup>†</sup>	10,500	52,800	42,300	30	Yes	37	Major	3	2	8–18
Irrawaddy, Myanmar	1,100	15,000	7,600	6,100	30	No	20	Moderate	2	1.4	3.4–6
Magdalena, Colombia	790	1,120	750	750	0	Yes	70	Moderate	6	3	5.3–6.6
Mekong, Vietnam	20,900	9,800	36,750	17,100	12	No	0	Moderate	0.5	0.4	6
Mississippi, USA	7,140 <sup>†</sup>	13,500	0	11,600	48	Yes	Unknown	Major	2	0.3	5–25
Niger, Nigeria	350 <sup>†</sup>	1,700	2,570	3,400	50	No	30	Major	0.6	0.3	7–32
Tigris <sup>‡</sup> , Iraq	9,700	1,730	770	960	50	Yes	38	Major	4	2	4–5
<b>Deltas in greater peril: virtually no aggradation and/or very high accelerated compaction</b>											
Chao Phraya, Thailand	1,780	800	4,000	1,600	85	Yes	30	Major	0.2	0	13–150
Colorado, Mexico	700	0; MP	0	0	100	Yes	0	Major	34	0	2–5
Krishna, India	250	840	1,160	740	94	Yes	0	Major	7	0.4	~3
Nile, Egypt	9,440	0; LP	0	0	98	Yes	75	Major	1.3	0	4.8
Pearl <sup>‡</sup> , China	3,720	1,040	2,600	520	67	Yes	0	Moderate	3	0.5	7.5
Po, Italy	630	0; LP	0	320	50	No	40	Major	3	0	4–60
Rhone, France	1,140	0; LP	920	0	30	No	40	Minor	7	1	2–6
Sao Francisco, Brazil	80	0; LP	0	0	70	Yes	0	Minor	2	0.2	3–10
Tone <sup>‡</sup> , Japan	410	220	0	160	30	Yes	§	Major	4	0	>10
Yangtze <sup>‡</sup> , China	7,080	6,700	3,330	6,670	70	Yes	0	Major	1.1	0	3–28
Yellow <sup>‡</sup> , China	3,420	1,430	0	0	90	Yes	80	Major	49	0	8–23

\* LP, little potential; MP, moderate potential; SP, significant potential.

<sup>†</sup> Significant canopy cover renders these SRTM elevation estimates conservative.

<sup>‡</sup> Alternative names: Congo and Zaire; Ganges and Ganges-Brahmaputra; Pearl and Zhujiang; Tigris and Tigris-Euphrates and Shatt al Arab; Tone and Edo; Yangtze and Changjiang; Yellow and Huanghe.

<sup>§</sup> The Tone has long had its flow path engineered, having once flowed into Tokyo Bay; the number of distributary channels has increased with engineering works.

navigation in the larger channels, plus the channels have become fixed in their location with levees to better protect populated areas from flooding<sup>1,5</sup>. In early human times, these distributary channels often changed their location and pattern (Fig. 3; Table 1). If the distributary channels are free to migrate across a delta plain, or episodically switch their position, widespread sedimentation occurs. Thirteen of the major deltas saw their distributary channel number decrease, some markedly (Table 1), with the Magdalena, Nile, Vistula, Yellow and Indus all showing major (70–80%) reductions.

The Indus provides a classic example of how, throughout the nineteenth century and earlier<sup>28</sup>, river distributary channels migrated across the delta surface (Fig. 3). SRTM topographic data reveal the lobate sediment deposits from the ancient crevasse splay and palaeo-river channels (Fig. 3a). Distributary channels were numerous, and successive surveys show channels to have been mobile (Fig. 3b). To use precious water resources better on the Indus floodplain, an elaborate irrigation system was put in place in the twentieth century (Fig. 3c) that captured much of the water, sediment and nutrients. Today very little water or sediment makes it to the delta plain through its remaining connection to the ocean (ref. 29; Table 1).

A few deltas have changed little across the twentieth century, and their aggradation rate remains in balance with, or exceeds, subsidence or relative sea-level rise (Table 1: Amazon, Congo, Fly, Orinoco, Mahakam). For most deltas, aggradation rates have either substantially decreased or been nearly eliminated (for example Chao Phraya, Colorado, Nile, Po, Tone, Vistula, Yangtze and Yellow). Sediment deposition is now mostly limited to fewer channels, where within-channel aggradation rates can be high (>60 mm yr<sup>-1</sup>; ref. 24) (Table 1), creating channels super-elevated above their surrounding flood plains and increasing the flood risk<sup>3,30</sup>. In the Nile Delta, the sediment escaping the upstream Aswan dam, which is already <2% of the original sediment load, is almost completely trapped by a dense network of irrigation channels in the delta<sup>31</sup>.

### Modern deltas below sea level

SRTM data reveal the extent and location of delta areas near or below sea level (Table 1). Our representative deltas have significant areas (>100,000 km<sup>2</sup>) of vulnerable lowlands at elevations less than 2 m above mean sea level (Table 1), and are thus susceptible to river floods and inundation from storm surges, especially those deltas subject to tropical storms (Supplementary Fig. S11). The SRTM altimetry (Table 1; Figs 1–3) has a vertical (root mean square) error between 1.1 m and 1.6 m in lowland areas (see ref. 32 and Supplementary Information). The deltas have a combined area of 26,000 km<sup>2</sup> below mean sea level (Fig. 1), protected from ambient coastal inundation by natural barriers (for example beach ridges and dunes), engineered structures or some combination of these (for example Po, Vistula, Nile and Yellow). The Pearl Delta, China, and the Mekong Delta, Vietnam, both inhabited by millions of people and exposed to typhoons, seem particularly at risk, with much of their surface area below mean sea level, and limited coastal barrier protection (Fig. 2). We calculate that the deltaic area at risk of flooding for these 33 deltas, given the IPCC estimates for projected sea-level rise<sup>10</sup>, would increase by 50% over the twenty-first century if global sea level continues to rise rapidly. In the Irrawaddy Delta, which has extensive lowlands, the coastal surge associated with Cyclone Nargis in 2008 inundated an area up to 6 m above sea level (Fig. 2). This makes it even more clear how conservative the areal estimates can be if high storm surges are involved in the flooding.

### The sinking of modern deltas

A few of our studied deltas seem not to be at risk; their aggradation rates are little changed, and they see little anthropogenic subsidence (Table 1: Amazon, Congo, Fly, Orinoco, Mahakam). Other deltas have seen their aggradation decrease across the twentieth century,

but the rate still exceeds the local  $\Delta_{\text{RSL}}$  (Table 1: Amur, Danube, Han and Limpopo). This condition offers a level of ongoing protection from storm-surge landward penetration. However, even a reduction in sediment delivery can trigger accelerating coastal erosion<sup>33,34</sup>.

Most of the deltas in Table 1 are now sinking at rates many times faster than global sea level is rising. In the table, three categories of deltas are identified, listed in order of increasing risk: (1) reduced aggradation that can no longer keep up with local sea-level rise (Brahmani, Godavari, Indus, Mahanadi, Parana, and Vistula); (2) reduced aggradation plus accelerated compaction overwhelming the rates of global sea-level rise (Ganges, Irrawaddy, Magdalena, Mekong, Mississippi, Niger and Tigris); (3) virtually no aggradation and/or very high accelerated compaction (for example Chao Phraya, Colorado, Krishna, Nile, Pearl, Po, Rhone, Sao Francisco, Tone, Yangtze and Yellow).

To keep the ocean off the landscape, coastlines are being strengthened through coastal barriers of untested strength. All trends point to ever-increasing areas of deltas sinking below mean sea level. Human occupation and infrastructure development continues, through the development of megacities and their expanding footprint on deltas. Early indications suggest that the magnitude and frequency of hurricanes and cyclones might increase<sup>35,36</sup> along with the onset of more intense precipitation events<sup>37</sup>. Although humans have largely mastered the everyday behaviour of lowland rivers, they seem less able to deal with the fury of storm surges that can temporarily raise sea level by 3 to 10 m. It remains alarming how often deltas flood, whether from land or from sea, and the trends seem to be worsening<sup>38</sup>.

### References

- Syvitski, J. P. M. & Saito, Y. Morphodynamics of deltas under the influence of humans. *Glob. Planet. Change* **57**, 261–282 (2007).
- Woodroffe, C. D., Nicholls, R. J., Saito, Y., Chen, Z. & Goodbred, S. L. in *Global Change and Integrated Coastal Management: The Asia-Pacific Region, Coastal Systems and Continental Margins* Vol. 10 (ed. Harvey, N.) 277–314 (Springer, 2006).
- Vörösmarty, C., Syvitski, J. P. M., Day, J., Paola, C. & Serebin, A. Battling to save the world's river deltas. *Bull. Atom. Sci.* **65**, 31–43 (2009).
- Nicholls, R. J. *et al.* in *IPCC Climate Change 2007: Impacts, Adaptation and Vulnerability* (eds Parry, M. L., Canziani, O. F., Palutikof, J. P., van der Linden, P. & Hanson, C. E.) 315–357 (Cambridge Univ. Press, 2007).
- Syvitski, J. P. M. Deltas at risk. *Sustain. Sci.* **3**, 23–32 (2008).
- Nicholls, R. J. Coastal flooding and wetland loss in the 21st century: Changes under the SRES climate and socio-economic scenarios. *Glob. Environ. Change* **14**, 69–86 (2004).
- Day, J. W. Jr *et al.* Restoration of the Mississippi Delta: Lessons from hurricanes Katrina and Rita. *Science* **315**, 1679–1684 (2007).
- Turner, R. E., Swenson, E. M., Milan, C. S. & Lee, J. M. Hurricane signals in salt marsh sediments: Inorganic sources and soil volume. *Limnol. Oceanogr.* **52**, 1231–1238 (2007).
- Turner, R. E., Baustian, J. J., Swenson, E. M. & Spicer, J. S. Wetland sedimentation from hurricanes Katrina and Rita. *Science* **314**, 449–452 (2006).
- Bindoff, N. L. *et al.* in *IPCC Climate Change 2007: The Physical Science Basis*. (eds Solomon, S. *et al.*) 385–433 (Cambridge Univ. Press, 2007).
- Church, J. A. & White, N. J. A 20<sup>th</sup> century acceleration in global sea-level rise. *Geophys. Res. Lett.* **33**, L01602 (2006).
- Milne, G. A., Gehrels, W. R., Hughes, C. W. & Tamisiea, M. E. Identifying the causes of sea-level change. *Nature Geosci.* **2**, 471–478 (2009).
- Meckel, T. A., Ten Brink, U. S. & Williams, S. J. Sediment compaction rates and subsidence in deltaic plains: Numerical constraints and stratigraphic influences. *Basin Res.* **19**, 19–31 (2007).
- Törnqvist, T. E. *et al.* Mississippi Delta subsidence primarily caused by compaction of Holocene strata. *Nature Geosci.* **1**, 173–176 (2008).
- Saito, Y., Chaimanee, N., Jarupongsakul, T. & Syvitski, J. P. M. Shrinking megadeltas in Asia: Sea-level rise and sediment reduction impacts from case study of the Chao Phraya Delta. *Inprint Newsletter of the IGBP/IHDP Land Ocean Interaction in the Coastal Zone* **2007/2**, 3–9 (2007).
- Caputo, M., Pieri, L. & Ungghendoli, M. Geometric investigation of the subsidence in the Po Delta. *Boll. Geofis. Teor. Appl.* **14**, 187–207 (1970).



17. Jouet, G., Hutton, E. W. H., Syvitski, J. P. M., Rabineau, M. & Berné, S. Modeling the isostatic effects of sealevel fluctuations on the Gulf of Lions. *Comput. Geosci.* **34**, 1338–1357 (2008).
18. Ivins, E. R., Dokka, R. K. & Blom, R. G. Post-glacial sediment load and subsidence, in coastal Louisiana. *Geophys. Res. Lett.* **34**, L16303 (2007).
19. Milne, G. A. & Mitrovica, J. X. Searching for eustasy in deglacial sea-level histories. *Quat. Sci. Rev.* **27**, 2292–2302 (2008).
20. Dokka, R. K., Sella, G. F. & Dixon, D. H. Tectonic control of subsidence and southward displacement of southeast Louisiana with respect to stable North America. *Geophys. Res. Lett.* **33**, L23308 (2006).
21. Blum, M. D., Tomkin, J. H., Purcell, A. & Lancaster, R. R. Ups and downs of the Mississippi Delta. *Geology* **36**, 675–678 (2008).
22. Hutton, E. W. H. & Syvitski, J. P. M. SedFlux2.0: New advances in the seafloor evolution and stratigraphic modular modeling system. *Comput. Geosci.* **34**, 1319–1337 (2008).
23. Dixon, T. H. Earth scientists and public policy: Have we failed New Orleans? *Eos* **89**, 96 (2008).
24. Syvitski, J. P. M., Kettner, A. J., Correggiari, A. & Nelson, B. W. Distributary channels and their impact on sediment dispersal. *Mar. Geol.* **222–223**, 75–94 (2005).
25. Milliman, J. D. & Syvitski, J. P. M. Geomorphic/tectonic control of sediment discharge to the ocean: The importance of small mountainous rivers. *J. Geol.* **100**, 525–544 (1992).
26. Syvitski, J. P. M. & Milliman, J. D. Geology, geography and humans battle for dominance over the delivery of sediment to the coastal ocean. *Geology* **115**, 1–19 (2007).
27. Roldolfo, K. S. & Siringan, F. P. Global sea-level rise is recognised, but flooding from anthropogenic land subsidence is ignored around northern Manila Bay, Philippines. *Disasters* **30**, 118–139 (2006).
28. Holmes, D. A. The recent history of the Indus. *Geog. J.* **134**, 367–382 (1968).
29. Giosan, L. *et al.* Recent morphodynamics of the Indus delta shore and shelf. *Cont. Shelf Res.* **26**, 1668–1684 (2006).
30. Han, M., Hou, J. & Wu, L. Potential impacts of sea level rise on China's coastal environment and cities: A national assessment. *J. Coastal Res.* **14**, 79–90 (1995).
31. Stanley, J. D. & Warne, A. G. Nile Delta in its destructive phase. *J. Coastal Res.* **14**, 794–825 (1998).
32. Schumann, G. *et al.* Comparison of remotely sensed water stages from LiDAR, topographic contours and SRTM. *ISPRS J. Photogram. Remote Sensing* **63**, 283–296 (2008).
33. Giosan, L. *et al.* Young Danube delta documents stable Black Sea level since the middle Holocene: Morphodynamic, paleogeographic, and archaeological implications. *Geology* **34**, 757–760 (2006).
34. Giosan, L., Bokuniewicz, H. J., Panin, N. & Postolache, I. Longshore sediment transport pattern along the Romanian Danube delta coast. *J. Coastal Res.* **15**, 859–871 (1999).
35. Goldenberg, S. B. *et al.* The recent increase in Atlantic hurricane activity: causes and implications. *Science* **293**, 474–479 (2001).
36. Holland, G. & Webster, P. Heightened tropical cyclone activity in the North Atlantic: Natural variability or climate trend? *Phil. Trans. R. Soc. A* **365**, 2695–2716 (2007).
37. Lambert, F. H., Stine, A. R., Krakauer, N. Y. & Chiang, J. C. H. How much will precipitation increase with global warming? *Eos* **89**, 193–194 (2008).
38. Overeem, I. & Syvitski, J. P. M. *Dynamics and Vulnerability of Delta Systems*. LOICZ Reports & Studies No. 35. (GKSS Research Center, 2009).

### Acknowledgements

We thank the following organizations for research funding: National Science Foundation (Cooperative Agreement 0621695), NASA (NNXOTAF2SG/P207124; NNXOTAF28G/P207124) and the Office of Naval Research (N00014-04-1-0235). Many scientists have contributed to this effort, including C. Paola (NCED), S. Peckham (CSDMS), W.-S. Kim (Univ. Illinois), J. Storms (Delft Univ. Technology) and I. Kelman (CICER).

### Additional information

Supplementary information accompanies this paper on [www.nature.com/naturegeoscience](http://www.nature.com/naturegeoscience).